Advances in Computational Mathematics (2023) 49:73
https://doi.org/10.1007/s10444-023-10072-w

An efficient approximation to the stochastic Allen-Cahn equation with random diffusion coefficient field and multiplicative noise

Xiao Qi[1] · **Yanrong Zhang**[1] · **Chuanju Xu**[1]

Received: 11 April 2023 / Accepted: 28 August 2023 / Published online: 27 September 2023

Abstract
This paper studies the stochastic Allen-Cahn equation involving random diffusion coefficient field and multiplicative force noise. A new time-stepping method based on auxiliary variable approach is proposed and analyzed. The proposed method is efficient thanks to its low computational complexity. Furthermore, it is unconditionally stable in the sense that a discrete energy is dissipative when the multiplicative noise is absent. Our numerical experiments show that the new scheme is much more robust than the classical semi-implicit Euler-Maruyama scheme, particularly when the interface width parameter is small. Several numerical examples are provided to demonstrate the performance of the proposed method.

Keywords Stochastic Allen-Cahn equation · Random coefficient · Multiplicative noise · Extended Euler-Maruyama scheme · Stability

Mathematics Subject Classification (2010) 60H15 · 60H35 · 65C50

1 Introduction

Stochastic partial differential equations (SPDEs) are widely used to mathematically model random phenomena occurring in the many fields of science and engineering, and have been subject of many theoretical and numerical investigations. It is commonly

Communicated by: Aihui Zhou

This research is partially supported by NSFC grant 11971408.

✉ Chuanju Xu
cjxu@xmu.edu.cn

[1] School of Mathematical Sciences and Fujian Provincial Key Laboratory of Mathematical Modeling and High Performance Scientific Computing, Xiamen University, Xiamen 361005, China

believed that incorporating noise and/or uncertainty into models is closer to reality in mathematical modeling. Over the past decades, there have been plenty of literature on the numerical study of stochastic evolution equations (SEEs); see, e.g., monographs [7, 31, 35, 41, 44, 58] and references therein. Although much progress has been made, the development of numerical techniques is still far from being satisfactory, especially for the SEEs with non-globally Lipschitz nonlinearity. Numerically solving SEEs may encounter the difficulties stemming from the nonlinearity, infinite dimensional operator, and driving noise; see, e.g., [8, 14, 15, 32, 33, 39, 45] and references therein.

A typical example of SEEs with non-globally Lipschitz nonlinearity is the stochastic Allen-Cahn equation. The Allen-Cahn equation was originally proposed by Allen and Cahn in [1] as a mathematical model to describe the phase separation process of a binary alloy quenched at a fixed temperature. Due to the existence of uncertainty stemming from various sources such as thermal fluctuation, impurities of materials and so on, it is often necessary to consider stochastic effects and to study the impact of noise on the phase change process. In fact the stochastic Allen-Cahn equation has attracted increasing attention in the past few years, see, e.g., [8–10, 22, 32, 33, 37, 40, 42, 45, 54] and references therein. There exists a large amount of literature on strong or weak convergence analysis of numerical schemes of the stochastic Allen-Cahn equations, which involves two error categories, namely weak error and strong error. The former is related to the approximation of the probability law of the solution. We refer to, e.g., [9–11, 13] and references therein for a list of literature on the weak error estimation of stochastic Allen-Cahn equations. Unlike weak error, the strong error measures the deviation from the trajectory of an exact solution. It has been extensively investigated for various types of the stochastic Allen-Cahn equations; see, e.g., [5, 6, 8, 13, 22, 25–28, 32, 33, 39, 40, 42, 45, 47, 55] and references therein. We mention here some works on strong convergence of the numerical approximations for stochastic Allen-Cahn equations with additive or multiplicative noise. For instance, Kovács et al. [33] proposed Euler type splitstep time scheme for the stochastic Allen-Cahn equation perturbed by smooth additive Gaussian noise, and showed that the strong convergence rate is $1/2$ with respect to the step size. Bréhier et al. [8] analyzed an explicit temporal splitting scheme for the stochastic Allen-Cahn equation driven by additive space-time white noise, and obtained optimal strong convergence rates of order $1/4$. Some other works related to strong error analysis of the stochastic Allen-Cahn equation with additive noise include Becker and Jentzen [6], Cui et al. [13], Qi et al. [45], and Wang [55], in which different schemes were constructed and analyzed. The case of strong convergence of stochastic Allen-Cahn equations with multiplicative noise is generally more subtle and challenging, and has received widely attention in the research community in recent years. For example, Feng et al. [22] proposed a finite element approximation to the stochastic Allen-Cahn equation with gradient-type multiplicative noise that is white in time and correlated in space. Majee et al. [42] investigated a modified spatio-temporal discretization to the stochastic Allen-Cahn equation with multiplicative noise and deduced uniform bounds in strong norms for this fully discrete scheme. There has also been work for more general SEEs with nonlinear terms which are not necessarily of the form of Allen-Cahn potential functional. In this regard, we mention the work by Jentzen et al. [28] on a method for approximating a class of semilinear stochastic equations with non-globally Lipschitz

continuous nonlinearities, and the work by Liu et al. [40] on a general theory of optimal strong error estimation for monotone drift driven by a multiplicative infinite-dimensional Wiener process.

The present work focuses on the numerical approximation of the stochastic Allen-Cahn equation with both multiplicative force noise and random diffusion coefficient field, which seems not yet been considered in the literature to the best of our knowledge. The aim is to propose and analyze efficient numerical methods for this equation. The idea is to make use of the auxiliary variable approach, which has been found useful in constructing stable schemes for gradient flows, and the popular Euler-Maruyama scheme for SEEs. Notice that Cui et al. [16] has proposed a similar idea for the stochastic wave equation with only multiplicative noise. The main contributions/novelties of this paper are summarized as follows:

- The well-posedness of the considered stochastic equation is established. That is, the existence, uniqueness, and the stability of the mild solution is proved.
- The diffusion coefficient considered in this current work is a log-Whittle-Matérn Gaussian random field with a parametrized covariance function whose regularity can be controlled by a parameter. Therefore, different cases can be tested and compared in a convenient way. A sampling approach called stochastic Fourier method [50, 51] is employed to render the equation solvable with determined diffusion coefficient field.
- The proposed time-stepping method is very efficient in term of the computational complexity and stability. The implementation detail shows that the computational complexity is equal to solving two second-order linear elliptic equations at each time step. The computational cost of this scheme is smaller than some drift-implicit Euler schemes [40, 42, 45] which require solving nonlinear equations at each time step. More advantageously, the time-stepping is unconditionally stable in the case the multiplicative noise is absent. Our numerical experiments show that the new scheme is much more stable compared to the classical semi-implicit Euler-Maruyama scheme [34, 46], especially when the interface width parameter is small.

The rest of paper is organized as follows. In Section 2, we establish the well-posedness of the considered problem under some standard assumptions. In Section 3, we briefly describe the sampling method for the random diffusion coefficient field, and present in details the spatio-temporal full discretization method. Several numerical examples are provided in Section 4 to demonstrate the performance of proposed method. In particular, a comparison with popular existing schemes is given.

2 Problem and its well-posedness

Let $T > 0$, $D \in \mathbb{R}^d$, $d \in \{1, 2, 3\}$, be a bounded open spatial domain with smooth boundary. To be specific, we consider $D := (0, 1)^d$ in this work. Let $L^2(D)$ and $H_0^\gamma(D)$ be classical Sobolev spaces, $\gamma \geq 0$. Let $(\cdot, \cdot)$ denote the $L^2(D)$-inner product and $\mathcal{L}(L^2(D))$ represent the space of bounded linear operators A: $L^2(D) \to L^2(D)$

equipped with operator norm $\|A\|_{\mathcal{L}(L^2(D))} = \sup_{u\neq 0} \frac{\|Au\|_{L^2(D)}}{\|u\|_{L^2(D)}}$. $(\Omega, \mathcal{F}, \{\mathcal{F}_t\}_{t\geq 0}, \mathbb{P})$ is a filtered probability space with a normal filtration $\{\mathcal{F}_t\}_{t\geq 0}$. We denote $v(x,\omega) \in L^2(\Omega, L^2(D))$ if

$$\|v\|_{L^2(\Omega,L^2(D))} < +\infty,$$

where the norm $\|v\|_{L^2(\Omega,L^2(D))}$ is defined by

$$\|v\|_{L^2(\Omega,L^2(D))} := \left(\mathbb{E}[\|v(\cdot,\omega)\|^2_{L^2(D)}]\right)^{\frac{1}{2}} \tag{2.1}$$

with $\mathbb{E}[\cdot]$ being the expectation in the probability space $(\Omega, \mathcal{F}, \mathbb{P})$. $L^2(\Omega, L^2(D))$ is also known as the space of the mean-square integrable random variables. Let $W(t,x)$ be a $\mathcal{F}_t$-adapted $H_0^\gamma(D)$-valued Wiener process with covariance operator Q, where Q is a positive definite and symmetric operator with orthonormal eigenfunctions $\{\phi_j(x) \in H_0^\gamma(D) : j \in \mathbb{N}\}$ and corresponding positive eigenvalues $\{q_j\}$; see, e.g., [32, 34, 53, 57] for more details.

Let $Q^{\frac{1}{2}}(H_0^\gamma(D)) := \{Q^{\frac{1}{2}}v : v \in H_0^\gamma(D)\}$. Let $\mathcal{L}_Q$ be the set of linear operators $B : Q^{\frac{1}{2}}(H_0^\gamma(D)) \to L^2(D)$, which satisfies

$$\left(\sum_{j=1}^{\infty} \|BQ^{\frac{1}{2}}\phi_j\|^2_{L^2(D)}\right)^{\frac{1}{2}} < +\infty.$$

$\mathcal{L}_Q$ endowed with the norm $\|B\|_{\mathcal{L}_Q} := \left(\sum_{j=1}^{\infty} \|BQ^{\frac{1}{2}}\phi_j\|^2_{L^2(D)}\right)^{\frac{1}{2}}$ is the space of Hilbert-Schmidt operators [23]. We will also use the space $L^2(\Omega, \mathcal{L}_Q)$ of all random Hilbert-Schmidt operators $B : \Omega \to \mathcal{L}_Q$, equipped with the norm

$$\|B(\omega)\|_{L^2(\Omega,\mathcal{L}_Q)} := \mathbb{E}[\|B(\omega)\|^2_{\mathcal{L}_Q}]^{\frac{1}{2}}.$$

Throughout the paper we use c, with or without subscripts, to mean generic positive constants (*independent of ω in particular*), which may not be the same at different occurrences.

We are interested in the stochastic Allen-Cahn equation written in the following abstract form:

$$\begin{aligned} du(x,t) &= (-Lu + f(u))dt + G(u)dW(x,t),\ 0 < t < T,\ x \in D,\\ u(x,t) &= 0,\quad 0 \leq t \leq T,\ x \in \partial D,\\ u(x,0) &= u_0(x),\ x \in \bar{D}, \end{aligned} \tag{2.2}$$

where $L := -\nabla\cdot(a(x,\omega)\nabla)$ is the elliptic operator with the coefficient $a(x,\omega)$ being a bounded log-Gaussian random field, i.e., there exists two constants $a_{\min}$ and $a_{\max}$

such that: for almost every $x \in \bar{D}$ and $\omega \in \Omega$,

$$0 < a_{\min} \leq a(x, \omega) = e^{z(x,\omega)} \leq a_{\max} < \infty. \tag{2.3}$$

Clearly the satisfaction of (2.3) relies on the uniform boundedness of the Gaussian random variable $z(x, \omega)$. Notice that (2.3) does not hold if $z(x, \omega)$ is Gaussian random variable without any restriction. Here we assume that for any $x \in \bar{D}$, $z(x, \omega)$ is a truncated Gaussian random variable [12, 29], such that $z_{\min} \leq z(x, \omega) \leq z_{\max}$ with $z_{\min}$ and $z_{\max}$ representing two constants. The uniform boundedness condition imposed on $a(x, \omega)$ guarantees that the constants produced in the subsequent analysis is independent of ω. It is worth to mention that the log-Gaussian random field has been used in the study of uncertainty quantification problems [3, 41], and appeared in some applications, e.g., geostatistical modelling [30, 52]. A more general model similar to problem (2.2) has been considered by Qi et al. [46], in which this kind of truncated Gaussian random variable is also used.

The nonlinear functional takes form $f(u) := -F'(u)$ with $F(u)$ being the Ginzburg-Landau double-well potential function, i.e.,

$$F(u) := \frac{1}{4\varepsilon^2}(u^2 - 1)^2, \tag{2.4}$$

where ε represents the scale parameter. It is known that this parameter controls the interface width, therefore also called the parameter thickness parameter. The theoretical result established in the paper depends on the following assumption on the nonlinear term $f(\cdot)$:

$$|f(u)| \leq c(1 + |u|), \qquad \max_{u \in R} |f'(u)| \leq c. \tag{2.5}$$

Obviously the satisfaction of the assumption (2.5) relies on the uniform boundedness of the solution u in D, which is a priori unknown. However, if u loses its boundedness in D, the truncation technique shown in paper [49] can be employed to restrict the growth of $F(u)$ to be quadratic when $|u|$ is bigger than a prescribed constant M, which is deterministic and independent of u. For example, it is common to replace the definition (2.4) by

$$F(u) = \begin{cases} \frac{3M^2-1}{2\varepsilon^2}u^2 - \frac{2M^3 u}{\varepsilon^2} + \frac{1}{4\varepsilon^2}(3M^4 + 1), & u > M, \\ \frac{1}{4\varepsilon^2}(u^2 - 1)^2, & u \in [-M, M], \\ \frac{3M^2-1}{2\varepsilon^2}u^2 + \frac{2M^3 u}{\varepsilon^2} + \frac{1}{4\varepsilon^2}(3M^4 + 1), & u < -M. \end{cases}$$

In this case, $f(u)$ becomes

$$f(u) = \begin{cases} -\frac{(3M^2-1)u}{\varepsilon^2} + \frac{2M^3}{\varepsilon^2}, & u > M, \\ \frac{u(1-u^2)}{\varepsilon^2}, & u \in [-M, M], \\ -\frac{(3M^2-1)u}{\varepsilon^2} - \frac{2M^3}{\varepsilon^2}, & u < -M. \end{cases} \tag{2.6}$$

It is clear from (2.6) that there exists a constant c such that (2.5) is satisfied.

We are interested in the mild solution of problem (2.2) in the Itô sense [17, 18], defined by

$$u(t) = S(t)u_0 + \int_0^t S(t-\tau)f(u(\tau))d\tau + \int_0^t S(t-\tau)G(u(\tau))dW(\tau), \quad (2.7)$$

where $S(t) := e^{-tL}$ is a semigroup generated by the operator L [21].

In order to establish the existence and uniqueness of a mild solution to (2.2), we furthermore assume that $z(x,\omega)$ is a $\mathcal{F}_0$-measurable, mean-zero, Whittle-Matérn Gaussian random field, which is a stationary random field with the covariance function

$$c_q(x) := \frac{g(\|x\|_2)}{2^{q-1}\Gamma(q)}, \ x \in \bar{D}, \ q > 2, \quad (2.8)$$

where $\Gamma(\cdot)$ is the Gamma function, and $g(\cdot)$ stands for the inverse Fourier transform of $\hat{g}(\xi) := \frac{2^{q-\frac{1}{2}}\Gamma(q+\frac{1}{2})}{(1+\xi^2)^{q+\frac{1}{2}}}$. It is known that the parameter q shown in (2.8) controls the regularity of the random field $z(x,\omega)$ [41]. Therefore, by taking different q value, it's easy to numerically test and compare different cases. Notice that the covariance function and mean function uniquely determine a Gaussian random field [41].

Some other assumptions on the nonlinear term G are also needed, which are collected below: - $L^s G(\cdot)$, $0 \le s \le 1/2$, is a mapping from $L^2(D)$ to $\mathcal{L}_Q$ such that:

$$\|L^s G(v)\|_{\mathcal{L}_Q} \le c\big(1 + \|v\|_{L^2(D)}\big), \ \ \forall v \in L^2(D), \quad (2.9)$$

$$\big\|L^s\big(G(v_1) - G(v_2)\big)\big\|_{\mathcal{L}_Q} \le c\|v_1 - v_2\|_{L^2(D)}, \ \ \forall v_1, v_2 \in L^2(D). \quad (2.10)$$

- $\{G(v(\tau)) : \tau \in [0,T]\}$ is a predictable $\mathcal{L}_Q$-valued process, such that

$$\int_0^T \mathbb{E}[\|G(v)\|^2_{\mathcal{L}_Q}]\, d\tau < +\infty, \ \forall v \in L^2(D). \quad (2.11)$$

We want to point out that, although these assumptions on the nonlinear term $G(\cdot)$ seem to be restrictive, the similar or more general assumptions have been considered in [2, 24, 34, 57], which are often used in establishing the existence and uniqueness of the solution to SPDEs.

The well-posedness of the problem (2.2) consists in verifying that the integrals in (2.7) are well defined and a function u satisfying the integral equation (2.7) uniquely exists. We first notice that the realization of the random field $a(x,\omega)$ given in (2.3) is 2 times mean-square differentiable due to $q > 2$ [41], and the domain of the operator L is $\mathcal{D}(L) = H^2(D) \cap H_0^1(D)$ almost surely [4]. We define the space $\mathbb{L}_2^t$ for $t \in [0,T]$,

which is the Banach space of $L^2(D)$-valued predictable processes $\{v(\tau) : \tau \in [0,t]\}$, equipped with the norm

$$\|v\|_{\mathbb{L}_2^t} := \sup_{\tau\in[0,t]} \|v(\tau)\|_{L^2(\Omega,L^2(D))} < +\infty.$$

Now we are in a position to state and prove the existence, uniqueness, and the stability of the mild solution (2.7). The proof is basically based on the framework of [41, Theorem 10.26], but adapted for the problem considered here. In particular, the randomness of the diffusion coefficient requires special care.

Theorem 2.1 *Suppose that the initial data $u_0 \in L^2(\Omega, L^2(D))$ is an $\mathcal{F}_0$-measurable random variable. Then, there exists a unique mild solution $u \in \mathbb{L}_2^T$ to (2.2). Furthermore, there exists a constant c_T depended on T such that the following stability inequality holds*

$$\|u\|_{\mathbb{L}_2^T} \le c_T(1 + \|u_0\|_{L^2(\Omega,L^2(D))}). \tag{2.12}$$

Proof We define the integral operator $\mathcal{M}$ by: for all $v \in \mathbb{L}_2^t$, $0 \le t \le T$,

$$(\mathcal{M}v)(t) := S(t)u_0 + \int_0^t S(t-\tau)f(v(\tau))d\tau + \int_0^t S(t-\tau)G(v(\tau))dW(\tau). \tag{2.13}$$

We emphasize here that the semigroup operator $S(\cdot)$ involves the random diffusion coefficient, thus the subsequent inequalities related to it should be understood in the sense of almost surely. Obviously if there is a fixed point $u \in \mathbb{L}_2^t$ for the operator $\mathcal{M}$, then this fixed point is a mild solution defined by (2.7). Now we will use the fixed point theorem to prove this is true by showing that $\mathcal{M}$ is a contraction mapping from $\mathbb{L}_2^{t_0} \to \mathbb{L}_2^{t_0}$ for small enough t_0.

1) First we prove that if $v \in \mathbb{L}_2^{t_0}$, then the integral operator $\mathcal{M}$ is well-defined, and $\mathcal{M}v \in \mathbb{L}_2^{t_0}$. Let $I_1(t) := \int_0^t S(t-\tau)G(v(\tau))dW(\tau)$. Using the Karhunen-Loève expansion of Q-Wiener process $W(\tau)$, Itô isometry, $\|S(t-\tau)\|_{\mathcal{L}(L^2(D))} \le 1$, and assumption (2.9) gives:

$$\|I_1(t)\|^2_{L^2(\Omega,L^2(D))} = \mathbb{E}[\|I_1(t)\|^2_{L^2(D)}] = \int_0^t \mathbb{E}\big[\|S(t-\tau)G(v)\|^2_{\mathcal{L}_Q}\big]d\tau \le \int_0^t \mathbb{E}[\|G(v)\|^2_{\mathcal{L}_Q}]d\tau < +\infty.$$

This means $I_1(t)$ is a predictable process and well defined in $L^2(\Omega, L^2(D))$. Moreover, it can be directly verified that $S(t)u_0$ and $\int_0^t S(t-\tau)f(v(\tau))d\tau$ are also predictable due to u_0 is $\mathcal{F}_0$-measurable and $v \in \mathbb{L}_2^{t_0}$. Therefore $(\mathcal{M}v)(t)$ is a predictable process.
We next show $\|\mathcal{M}v\|_{\mathbb{L}_2^t} < +\infty$, $0 \le t \le t_0$. Using $\|S(t)\|_{\mathcal{L}(L^2(D))} \le 1$ yields:

$$\|S(t)u_0\|_{L^2(\Omega,L^2(D))} \le \mathbb{E}\big[\|S(t)\|^2_{\mathcal{L}(L^2(D))}\|u_0\|^2_{L^2(D)}\big]^{\frac{1}{2}} \le \|u_0\|_{L^2(\Omega,L^2(D))} < +\infty.$$

Under the assumption (2.5), we have, for $v \in \mathbb{L}_2^{t_0}$,

$$\begin{aligned}\Big\| \int_0^t S(t-\tau) f(v) d\tau \Big\|_{L^2(\Omega, L^2(D))} &\le \int_0^t \|S(t-\tau) f(v)\|_{L^2(\Omega, L^2(D))} d\tau \\ &\le c \int_0^t (1 + \|v\|_{L^2(\Omega, L^2(D))}) d\tau < +\infty.\end{aligned}$$

By the Itô isometry, (2.9), the definition of $\|\cdot\|_{\mathcal{L}_Q}$, and $\int_0^t \|L^{-\frac{1}{2}} S(t-\tau)\|^2_{\mathcal{L}(L^2(D))} d\tau \le ct$ [41, Exercise 10.8], we obtain

$$\begin{aligned}\Big\| \int_0^t S(t-\tau) G(v) dW(\tau) \Big\|^2_{L^2(\Omega, L^2(D))} &= \int_0^t \mathbb{E}\big[\big\|L^{-\frac{1}{2}} S(t-\tau) L^{\frac{1}{2}} G(v(\tau))\big\|^2_{\mathcal{L}_Q}\big] d\tau \\ &\le c\mathbb{E}\Big[\int_0^t \big\|L^{-\frac{1}{2}} S(t-\tau)\big\|^2_{\mathcal{L}(L^2(D))} \big(1 + \|v\|_{L^2(D)}\big)^2 d\tau\Big] \\ &\le c\mathbb{E}\Big[\big(1 + \sup_{0\le\tau\le t} \|v(\tau)\|_{L^2(D)}\big)^2 \int_0^t \big\|L^{-\frac{1}{2}} S(t-\tau)\big\|^2_{\mathcal{L}(L^2(D))} d\tau\Big] \\ &\le ct\big(1 + \sup_{0\le\tau\le t} \|v(\tau)\|_{L^2(\Omega, L^2(D))}\big)^2 < +\infty.\end{aligned}$$

This shows that all terms in $(\mathcal{M}v)(t)$ are uniformly bounded in $[0, t_0]$ in the norm $\|\cdot\|_{L^2(\Omega, L^2(D))}$. Therefore $\|\mathcal{M}v\|_{\mathbb{L}_2^{t_0}} < +\infty$.

2) Then we prove that $\mathcal{M}$ is a contraction mapping on $\mathbb{L}_2^{t_0}$. A similar reasoning as above gives: for $0 \le t \le t_0$,

$$\begin{aligned}\|(\mathcal{M}v_1)(t) - (\mathcal{M}v_2)(t)\|^2_{L^2(\Omega, L^2(D))} &\le c\Big(\int_0^t \big\|S(t-\tau)\big(f(v_1(\tau)) - f(v_2(\tau))\big)\big\|_{L^2(\Omega, L^2(D))} d\tau\Big)^2 \\ &\quad + c\Big\|\int_0^t S(t-\tau)(G(v_1(\tau)) - G(v_2(\tau)))dW(\tau)\Big\|^2_{L^2(\Omega, L^2(D))} \\ &\le c\Big(\int_0^t \big\|f'\big(v_1 + \theta(v_2 - v_1)\big)\big(v_1(\tau) - v_2(\tau)\big)\big\|_{L^2(\Omega, L^2(D))} d\tau\Big)^2 \\ &\quad + c\int_0^t \mathbb{E}\big[\big\|L^{-\frac{1}{2}} S(t-\tau)\big\|^2_{\mathcal{L}(L^2(D))} \big\|L^{\frac{1}{2}}\big(G(v_1(\tau)) - G(v_2(\tau))\big)\big\|^2_{\mathcal{L}_Q}\big] d\tau \\ &\le ct^2 \sup_{0\le\tau\le t} \|v_1(\tau) - v_2(\tau)\|^2_{L^2(\Omega, L^2(D))} \\ &\quad + c\mathbb{E}\Big[\sup_{0\le\tau\le t} \|v_1 - v_2\|^2_{L^2(D)} \int_0^t \big\|L^{-\frac{1}{2}} S(t-\tau)\big\|^2_{\mathcal{L}(L^2(D))} d\tau\Big] \\ &\le c(t^2 + t)\|v_1(\tau) - v_2(\tau)\|^2_{\mathbb{L}_2^t},\end{aligned}$$

where $\theta \in (0, 1)$. Therefore we obtain

$$\|\mathcal{M}v_1 - \mathcal{M}v_2\|^2_{\mathbb{L}_2^{t_0}} \le c(t_0^2 + t_0)\|v_1 - v_2\|^2_{\mathbb{L}_2^{t_0}}.$$

It means $\mathcal{M}$ is a contraction mapping on $\mathbb{L}_2^{t_0}$ if $c(t_0^2 + t_0) < 1$, which is satisfied for small enough t_0. As a consequence, there exists a mild solution $u(t)$ to (2.2) in

$(0, t_0]$. Note that c that makes the inequality $c(t_0^2 + t_0) < 1$ hold is independent of the initial value u_0, thus one can repeat the above proof on the time interval $[t_0, 2t_0]$, $[2t_0, 3t_0]$ and so on to show that there exists a mild solution $u(t)$ to (2.2) in $(0, T]$.

3) Finally, we prove the stability inequality (2.13). We can likewise show that there exists a constant $c_T > 0$ depending on T such that

$$\|u(t)\|^2_{L^2(\Omega,L^2(D))} \leq c_T\big((1+\|u_0\|_{L^2(\Omega,L^2(D))})^2+\int_0^t \|u(\tau)\|^2_{L^2(\Omega,L^2(D))}d\tau\big), \quad \forall t \in (0, T].$$

Then using Gronwall's inequality gives

$$\sup_{t\in[0,T]} \|u(t)\|_{L^2(\Omega,L^2(D))} \leq c_T(1 + \|u_0\|_{L^2(\Omega,L^2(D))}).$$

This completes the proof. □

3 Stochastic Fourier sampling and fully discrete scheme

In this section, we aims to propose a sampling method to sample the random diffusion coefficient field $a(x, \omega)$. The proposed method is the so-called stochastic Fourier approach (also known as quadrature method) [50, 51]. It is worthwhile to point out that some other sampling methods, such as turning bands method [19, 43] and circulant embedding with padding method [20, 56], are also available. However the turning bands method is only applicable to isotropic Gaussian random fields, and the computational cost of the circulant embedding method is too large in high dimensions. One of the merit of the sampling method we employ here is its applicability to stationary Gaussian random fields including isotropic random fields, and its computational cost is roughly equal to computing a stochastic Fourier integral.

It is obvious from (2.3) that if we want to sample $a(x, \omega)$, we only need to sample $z(x, \omega)$. The crucial ingradient of the stochastic Fourier method is to construct a new random field that is the same as $z(x, \omega)$ in the sense of distribution through stochastic Fourier integral, and then approximately calculate the constructed random field by numerical integration to sample $z(x, \omega)$ indirectly. We will briefly describe this approach by taking one-dimensional sampling as an example in this section. Another purpose in this section is to propose and analyze a finite element method and time stepping scheme for spatio-temporal discretization of the problem (2.2). We start with the stochastic Fourier sampling.

3.1 Stochastic Fourier sampling

Consider the sampling of the random field $z(x, \omega)$ for $x \in [0, 1]$. It is known from (2.8) that the covariance function of the random field $z(x, \omega)$ is stationary, thus one

gets easily from the Wiener-Khintchine theorem [41, Theorem 6.5] that

$$c_q(x) = \int_{\mathbb{R}} e^{i\xi x} f_s(\xi) d\xi, \quad x \in [0, 1],$$

where $f_s(\xi)$ stands for the spectral density function corresponding to $c_q(x)$. Then using (2.8) and the Fourier transform gives

$$f_s(\xi) = \frac{\hat{g}(\xi)}{2^{q-1}\Gamma(q)\sqrt{2\pi}} = \frac{\Gamma(q+\frac{1}{2})}{\Gamma(q)\Gamma(\frac{1}{2})} \frac{1}{(1+\xi^2)^{q+\frac{1}{2}}}. \tag{3.1}$$

Let $\{\mathcal{W}(\xi) : \xi \in \mathbb{R}\}$ be a complex Brownian motion, i.e., $\mathcal{W}(\xi) := W_1(\xi) + iW_2(\xi)$ with $W_1(\xi)$ and $W_2(\xi)$ representing independent two-sided Brownian motions. Combining $\mathcal{W}(\xi)$ and $f_s(\xi)$ allows to construct a new random field $Z(x)$ defined by

$$Z(x) := \int_{\mathbb{R}} e^{ix\xi} \sqrt{f_s(\xi)} d\mathcal{W}(\xi). \tag{3.2}$$

It is readily obtained that

$$\mathbb{E}[Z(x)\bar{Z}(y)] = 2\int_{\mathbb{R}} e^{ix\xi} \sqrt{f_s(\xi)}\, e^{-iy\xi} \sqrt{f_s(\xi)} d\xi = 2\int_{\mathbb{R}} e^{i(x-y)\xi} f_s(\xi) d\xi. \tag{3.3}$$

Notice that $f_s(\xi)$ given in (3.1) is an even function of ξ, thus both $\int_{\mathbb{R}} e^{i(x-y)\xi} f_s(\xi) d\xi$ and $\mathbb{E}[Z(x)\bar{Z}(y)]$ are real. It follows from (3.3) and [41, Corollary 6.27] that $Z(x)$ is a stationary complex Gaussian random field with mean-zero and covariance $2c_q(x)$. Consequently the real and imaginary parts of $Z(x)$ are independent copies of a real-valued stationary Gaussian random field with mean-zero and covariance $c_q(x)$. This means that the real and imaginary parts of $Z(x)$ have the same distribution as our target random field $z(x, \omega)$ shown in (2.3). Hence, the stochastic Fourier integral (3.2) provides a way to sample $z(x, \omega)$ through approximating $Z(x)$ by numerical integral. For example, we can approximate $Z(x)$ by the trapezoid rule as follows:

$$Z(x) \approx \sum_{j=0}^{J} e^{ix\xi_j} \sqrt{f_s(\xi_j)} \Delta\mathcal{W}_j, \tag{3.4}$$

where $\xi_j = -R + j\Delta\xi$, $j = 0, 1, \ldots, J$, $\Delta\xi = \frac{2R}{J}$ with R being a large enough number,

$$\Delta\mathcal{W}_j := \begin{cases} \mathcal{W}(\xi_0 + \frac{\Delta\xi}{2}) - \mathcal{W}(\xi_0), & j = 0, \\ \mathcal{W}(\xi_j + \frac{\Delta\xi}{2}) - \mathcal{W}(\xi_j - \frac{\Delta\xi}{2}), & j = 1, ..., J-1, \\ \mathcal{W}(\xi_J) - \mathcal{W}(\xi_J - \frac{\Delta\xi}{2}), & j = J. \end{cases}$$

It is seen from the above definition that $\Delta\mathcal{W}_j \sim \mathrm{CN}(0, 2\Delta\xi)$ for $j = 1, ..., J-1$ and $\Delta\mathcal{W}_j \sim \mathrm{CN}(0, \Delta\xi)$ for $j = 0$ and J, where $\mathrm{CN}(\cdot, \cdot)$ stands for complex Gaussian

distribution [41, Definition 6.15]. Hence, for a given x, $Z(x)$ can be easily sampled because $\Delta\mathcal{W}_j$ are pairwise independent, and its real or imaginary part can be used as an approximation to $z(x, \omega)$.

Note that the sampling method described above is convenient in the sense that it only needs to numerically compute a stochastic Fourier integral and can simultaneously produce two sets of independent and identically distributed (i.i.d) samples in one sampling. Notably, for each of the sampling data of the random diffusion coefficient, the problem (2.2) becomes a stochastic Allen-Cahn equation with randomness only on the $G(\cdot)$-term. The forthcoming subsections will focus on the spatio-temporal full discretization of the problem (2.2).

3.2 A time stepping scheme based on auxiliary variable approach

The proposed time scheme makes use of an auxiliary variable approach, known as SAV, originally introduced by Shen et al. in [48] for deterministic gradient flows. Although this approach has been successfully applied to construct efficient schemes for a large class of nonlinear problems, its generalization to stochastic equations needs some care, especially when the differentiation of random fields is involved. The idea is to introduce the time-dependent auxiliary variable $r(t) := \sqrt{\int_D F(u)dx + c_0}$ for each $\omega \in \Omega$, c_0 is a positive constant such that $\int_D F(u)dx + c_0$ is positive. Then we insert this auxiliary variable into the original equation (2.2), yielding the following equivalent reformulation:

$$\begin{aligned} du(t) &= -\mu(t)dt, \ t \in (0, T), \ x \in D, \\ \mu(t) &= Lu - \frac{r(t)}{\sqrt{\int_D F(u)dx + c_0}} f(u) - G(u)\dot{W}(t, x), \\ dr(t) &= -\frac{\int_D f(u)\partial_t u(t)\, dx}{2\sqrt{\int_D F(u)dx + c_0}} dt, \end{aligned} \tag{3.5}$$

where $\dot{W}(t, x)$ is the white noise, which is the time derivative of the Q-Wiener process $W(t, x)$, i.e., $\dot{W}(t, x)dt = dW(t, x)$. Note that in the above reformulation, although all the unknown variables u, μ, and r are denoted as functions of t, u, and μ are indeed also functions of x too. Two facts are readily seen: (i) the equation sets (2.2) and (3.5) are strictly equivalent at the continuous level; (ii) the equation set (3.5) looks more complicated with an additional variable r as compared to the original one (2.2). However, as we are going to see, starting with the reformulation (3.5), it becomes much easier to construct stable schemes. Recently, this type of approaches has been considered and applied to solve stochastic wave equation with multiplicative noise by Cui et al. [16]. We believe it is interesting to see the potential advantage of this approach in approximating other SPDEs such as the equation considered in the current paper.

The time stepping method we propose reads:

$$\begin{aligned} u^{n+1}-u^n &= -\Delta t\mu^{n+1},\\ \mu^{n+1} &= Lu^{n+1}-\frac{r^{n+1}}{\sqrt{\int_D F(u^n)dx+c_0}}f(u^n)-G(u^n)\frac{\Delta W^n}{\Delta t},\\ \frac{r^{n+1}-r^n}{\Delta t} &= -\frac{1}{2\sqrt{\int_D F(u^n)dx+c_0}}\int_D f(u^n)\frac{u^{n+1}-u^n}{\Delta t}dx, \end{aligned} \tag{3.6}$$

where $\Delta t = \frac{T}{N}$ is the uniform time step size for a positive integer N, u^n is the time discrete approximation to $u(t_n)$ for $t_n = n\Delta t$, and $\Delta W^n := W(t_{n+1}) - W(t_n)$. Essentially, the above scheme is a kind of Euler-Maruyama discretization [34, 41, 46] applied to the reformulation system (3.5), will thus be termed as "extended Euler-Maruyama scheme" hereafter.

One remarkable property of the above scheme is that it satisfies an energy dissipation law in the absence of multiplicative noise, as shown in the following proposition. This dissipation law implies that the proposed scheme is unconditionally stable because the numerical solution remains bounded during the time stepping.

Proposition 3.1 (Unconditional stability) *Without the source term, i.e., $G(\cdot) = 0$, the numerical solution of the discrete problem (3.6) satisfies the following energy dissipation law for almost every $\omega \in \Omega$:*

$$E^{n+1} \le E^n, \quad \forall n = 0, 1, \ldots, N-1, \tag{3.7}$$

where $E^{n+1} := \frac{1}{2}\left\|\sqrt{a(x,\omega)}\nabla u^{n+1}\right\|^2_{L^2(D)} + |r^{n+1}|^2$.

Proof For almost every $\omega \in \Omega$, taking the $L^2(D)$-inner product $(\cdot,\cdot)$ of the first and second equations of (3.6) with μ^{n+1} and $(u^{n+1}-u^n)$ respectively, and multiplying the third equation by $2r^{n+1}$, then summing up the resulting equations, we obtain

$$\left(\sqrt{a(x,\omega)}\nabla u^{n+1}, \sqrt{a(x,\omega)}\nabla(u^{n+1}-u^n)\right) + 2(r^{n+1}, r^{n+1}-r^n) = -\Delta t(\mu^{n+1},\mu^{n+1}).$$

Using the identity $b^{n+1}(b^{n+1}-b^n) = \frac{1}{2}(|b^{n+1}|^2 - |b^n|^2 + |b^{n+1}-b^n|^2)$ gives:

$$E^{n+1} - E^n + \frac{1}{2}\left\|\sqrt{a(x,\omega)}(\nabla u^{n+1}-\nabla u^n)\right\|^2_{L^2(D)} + |r^{n+1}-r^n|^2 = -\Delta t(\mu^{n+1},\mu^{n+1}).$$

Thus

$$E^{n+1} - E^n \le -\Delta t(\mu^{n+1},\mu^{n+1}) \le 0.$$

This completes the proof. □

The scheme can be very efficiently implemented by using a suitable decomposition technique, which we describe below. It follows from the first and second equations of (3.6) that

$$u^{n+1} := u_1^{n+1} + r^{n+1} u_2^{n+1}, \tag{3.8}$$

where u_1^{n+1} or u_2^{n+1} solves the following elliptic equation

$$(I + \Delta t L)u = g^n \ \text{ in } D \tag{3.9}$$

with the source term g^n being $g_1^n := u^n + G(u^n)\Delta W^n$ and $g_2^n := \Delta t \frac{f(u^n)}{\sqrt{\int_D F(u^n)dx + c_0}}$ respectively. Obviously, u_1^{n+1} and u_2^{n+1} can be separately solved through the elliptic equation (3.9). It now remains to compute r^{n+1}. This can be done by plugging (3.8) into the third equation of (3.6), which gives

$$\Big(1 + \frac{\int_D f(u^n) u_2^{n+1} dx}{2\sqrt{\int_D F(u^n)dx + c_0}}\Big) r^{n+1} = r^n - \frac{\int_D f(u^n)(u_1^{n+1} - u^n)dx}{2\sqrt{\int_D F(u^n)dx + c_0}}.$$

Once r^{n+1} is computed from this equation, inserting it into (3.8) gives u^{n+1}.

It is seen that the overall cost of the proposed scheme (3.6) is roughly equal to solving two decoupled second-order equations with random coefficients at each time step. In the following, we briefly describe the spatial discretization.

3.3 Spatial discretization

Consider the $\mathbb{P}_1$ finite element method for the spatial discretization of the problem (3.6). Let $\mathcal{T}_h$ be a regular triangulation. Define the finite element space V_h by

$$V_h := \{v \in C^0(\bar{D}),\ v = 0 \text{ on } \partial D,\ v|_K \in \mathbb{P}_1(K) \text{ for all } K \in \mathcal{T}_h\},$$

where $\mathbb{P}_1(K)$ denotes the space of the polynomials of degree ≤ 1 defined in K. Let $\mathcal{P}_h$ be the orthogonal projection from $L^2(D)$ to V_h, and $\mathcal{P}_J^w$ be the projection from $H_0^\gamma(D)$ to the finite-dimensional space $\text{span}\{\phi_1, \ldots, \phi_J\}$. Set the initial condition to be $u_h^0 := \mathcal{P}_h u_0$ and the initial auxiliary variable to be $r_h^0 := \sqrt{\int_D F(u_h^0)dx + c_0}$.

Given the previous step solution $u_h^n \in V_h$, $r_h^n \in \mathbb{R}$, the spatial discretization of the problem (3.6) reads: find $u_h^{n+1} \in V_h$, $r_h^{n+1} \in \mathbb{R}$, such that for each $\omega \in \Omega$, $v_h \in V_h$, and $n = 0, \cdots, N-1$,

$$\begin{aligned}
(u_h^{n+1} - u_h^n, v_h) &= -\Delta t(\mu_h^{n+1}, v_h),\\
(\mu_h^{n+1}, v_h) &= \big(a(x,\omega)\nabla u_h^{n+1}, \nabla v_h\big) - \frac{r_h^{n+1}}{\sqrt{\int_D F(u_h^n)dx + c_0}}(f(u_h^n), v_h) - \frac{1}{\Delta t}\big(G(u_h^n)\mathcal{P}_J^w \Delta W^n, v_h\big),\\
r_h^{n+1} - r_h^n &= -\frac{1}{2\sqrt{\int_D F(u_h^n)dx + c_0}} \int_D f(u_h^n)(u_h^{n+1} - u_h^n)dx,
\end{aligned} \tag{3.10}$$

where $\mathcal{P}_J^w \Delta W^n := \sum_{j=1}^J \sqrt{q_j}(\beta_j(t_{n+1}) - \beta_j(t_n))\phi_j$ with $\beta_j(t)$ representing the i.i.d $\mathcal{F}_t$-Brownian motions.

The full discrete scheme (3.10) can be realized through solving $u_h \in V_h$ from the following elliptic problem:

$$\big(u_h, v_h\big) + \Delta t\big(a(x,\omega)\nabla u_h, \nabla v_h\big) = \big(g_h^n, v_h\big), \quad \forall v_h \in V_h, \tag{3.11}$$

where

$$g_h^n = u_h^n + G(u_h^n)\mathcal{P}_J^w \Delta W^n \tag{3.12}$$

or

$$g_h^n = \frac{\Delta t}{\sqrt{\int_D F(u_h^n)dx + c_0}} f(u_h^n). \tag{3.13}$$

We separately denote by $u_{1,h}^{n+1}$ and $u_{2,h}^{n+1}$ the solution of (3.11) for g_h^n in (3.12) and (3.13), then the current step solution u_h^{n+1} is obtained by

$$u_h^{n+1} = u_{1,h}^{n+1} + r_h^{n+1} u_{2,h}^{n+1}, \tag{3.14}$$

where r_h^{n+1} is computed by

$$\Big(1 + \frac{\int_D f(u_h^n)u_{2,h}^{n+1}dx}{2\sqrt{\int_D F(u_h^n)dx + c_0}}\Big) r_h^{n+1} = r_h^n - \frac{\int_D f(u_h^n)(u_{1,h}^{n+1} - u_h^n)dx}{2\sqrt{\int_D F(u_h^n)dx + c_0}}. \tag{3.15}$$

To summarize, the ful discrete scheme (3.10) can be implemented as follows:

i) Solve $u_{1,h}^{n+1}$ and $u_{2,h}^{n+1}$ from (3.11) for g_h^n defined in (3.12) and (3.13) respectively;
ii) Compute r_h^{n+1} by (3.15);
iii) Compute u_h^{n+1} by (3.14).

In actual calculation, we will use the average of the sampled values at the finite element nodes to approximate $a(x, \omega)$.

4 Numerical experiments

Several numerical examples are presented in this section to demonstrate the performance of the proposed scheme and show the effect of stochastic factors on numerical solutions. We start by testing the convergence orders of the temporal and spatial discretization.

Example 4.1 (Accuracy and stability test) We take the following one-dimensional stochastic Allen-Cahn equation with random diffusion coefficient field and multiplicative force noise:

$$\begin{aligned} du(x,t) &= \partial_x\left(e^{z(x,\omega)}\partial_x u\right)dt + \frac{u-u^3}{\varepsilon^2}dt + G(u)dW(x,t),\ 0<t<T,\ x\in(0,1),\\ u(0,t) &= u(1,t) = 0,\quad 0\le t\le T,\\ u(x,0) &= u_0(x),\ x\in(0,1), \end{aligned} \tag{4.1}$$

where $z(x,\omega)$ is the truncated Gaussian random field with mean-zero and covariance function $c_q(x)$, and $W(x,t)$ is a H_0^γ-valued Wiener process defined by

$$W(x,t) = \sum_{j=1}^{\infty}\sqrt{q_j}\sin(j\pi x)\beta_j(t), \tag{4.2}$$

where $q_j = \mathcal{O}(j^{-(2\gamma+1+\epsilon)})$ with arbitrary small positive ϵ.

We first test the effectiveness of the sampling method used in this paper. For each $x\in\bar{D}$, denote by $\mu_m(x)$ the approximation of $\mathbb{E}[z(x,\omega)]$ under m samples. We run the sampling method presented in Section 3.1 to produce an approximation of the random vector $\boldsymbol{z} = \left(z(x_1,\omega),\ldots,z(x_P,\omega)\right)^T$ by taking $P = 100$ and $q = 3$. Furthermore we calculate $|\mu_m(x)|$ for $x = 0.1, 0.5, 0.9$ and $m = 10, 20, 50, 100$. The obtained result is shown in Fig. 1, from which we observe that as the sampling number increases, $|\mu_m(x)|$ converges to the theoretical mean-zero, and the convergence rate is roughly $O(m^{-\frac{1}{2}})$.

We then test the time-space strong convergence rate of the full discrete scheme, where the strong convergence is understood in the sense of convergence with respect

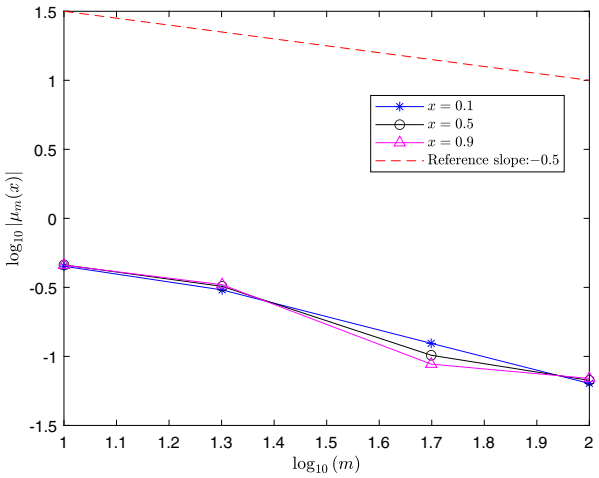

Fig. 1 Mean of sample values $|\mu_m(x)|$ as function of m in log-log scale

to the norm $\|\cdot\|_{L^2(\Omega,L^2(D))}$. In particular, we will compare the result to that of the classical semi-implicit Euler-Maruyama scheme, i.e., find $u_h^{n+1} \in V_h$, such that

$$\begin{aligned}(I + \Delta t L_h)u_h^{n+1} &= u_h^n + \Delta t \mathcal{P}_h f(u_h^n) + \mathcal{P}_h\big(G(u_h^n)\mathcal{P}_J^w \Delta W^n\big),\ n = 0, \cdots, N-1,\\ u_h^0 &= \mathcal{P}_h u_0,\end{aligned} \tag{4.3}$$

where $L_h\colon V_h \to V_h$ is the finite-dimensional operator defined by

$$(L_h w, v) := (a(x,\omega)\nabla w, \nabla v),\quad \forall w, v \in V_h.$$

It is worth pointing out that the strong convergence analysis of the stochastic Allen-Cahn equation is generally more difficult than that of the SPDEs with globally Lipschitz nonlinearity due to the presence of the non-globally Lipschitz (cubic) nonlinearity of the Allen-Cahn potential functional, see, e.g., [5, 9, 45, 55]. Although no error analysis for the FEM/extended Euler-Maruyama scheme (3.10) is available, we notice that under the assumption (2.5), the strong error estimate of the scheme (4.3) has been derived in our recent paper [46]. In that paper the strong convergence rate $\mathcal{O}(h^{2-\delta} + \Delta t^{\frac{1}{2}})$ was proved for the scheme (4.3), where δ is an infinitesimal number. This numerical test has the purpose of checking if the scheme (3.6) is more stable than (4.3), while they have comparable accuracy.

The strong convergence rate in time and space is measured in terms of mean-square approximation errors at the endpoint $T = 0.001$. Since the exact solution of the problem (4.1) is unknown, we will use the reference solution computed in a finer time-space mesh as the exact solution. Precisely, the "exact solution" is computed by using $h = 1/128$ and $\Delta t = 10^{-8}$ in the time accuracy test, and $h = 1/512$ and $\Delta t = 10^{-6}$ in the spatial accuracy test. The error expectation, denoted by u_{error}, is approximated by computing the mean of 200 samples: $\left(\frac{1}{200}\sum_{j=1}^{200}\|u_j^{\text{ref}} - u_{j,h}^N\|_{L^2(D)}^2\right)^{\frac{1}{2}}$, where u_j^{ref} and $u_{j,h}^N$ are respectively the exact solution and the approximative solution for the j-th sample.

We calculate u_{error} with different time steps and mesh sizes by taking $u_0(x) = \sin(2\pi x)$, $\varepsilon = 1$, $c_0 = 0$, $\gamma = 2$ and $q = 2$. The error behavior with respect to the time step size and the finite element mesh size is presented in Table 1 for $G(u) = 5(1-u^2)$. Also shown is the comparison between the classical semi-implicit and our new scheme. The same test is repeated for $G(u) = 5u$, and the result is given in Table 2. It is observed in these tables that both the classical semi-implicit and the new schemes give the same convergence rate, 1/2-order in time and second order in space as expected.

Next, we focus on the stability comparision of the extended Euler-Maruyama scheme (3.6) and classical semi-implicit scheme (4.3). Consider the model (4.1) again. Fix a random stream, take $u_0 = \sin(4\pi x)$, $\gamma = 1$, $c_0 = 0$, $q = 2$, $G(u) = (1-u^2)/2$, $h = 1/64$, $T = 1$, $\varepsilon = 0.01$. We run the both schemes with different time steps, and trace the evolution of the numerical solution u_h^N. We say the scheme blows up if we get a NaN for the numerical solution. We find that when $\Delta t \geq 2.2 \times 10^{-4}$, the

Table 1 Time (upper table) and space (lower table) convergence rates with $G(u) = 5(1 - u^2)$

	Semi-implicit		New scheme	
	u_{error}	Order	u_{error}	Order
Time step Δt				
1.00E-4	3.25E-3	-	3.31E-3	-
5.00E-5	2.38E-3	0.45	2.57E-3	0.37
2.50E-5	1.75E-3	0.44	1.85E-3	0.47
1.25E-5	1.27E-3	0.47	1.23E-3	0.58
6.25E-6	9.17E-4	0.47	8.89E-4	0.47
Mesh size h				
1/16	1.05E-2	-	1.06E-3	-
1/32	2.70E-3	1.96	2.70E-3	1.97
1/64	6.88E-4	1.97	7.02E-4	1.94
1/128	1.76E-4	1.97	1.80E-4	1.97
1/256	4.28E-5	2.04	4.51E-5	2.00

semi-implicit Euler-Maruyama scheme blows up at time $t = 2.42 \times 10^{-3}$, whereas the new scheme allows stable long time calculation (stoped at $t = 390$) even for the time step $\Delta t = 10^{-1}$. We also test the stability for the problem (4.1) with the nonlinear drift term $\frac{u-u^3}{\varepsilon^2}$ replaced by $-\frac{u}{\varepsilon^2}$ and keeping other terms and inputs unchanged. The computed result shows that when $\Delta t \geq 2.1 \times 10^{-4}$, the traditional semi-implicit scheme blows up at time $t = 2.46 \times 10^{-2}$, while the new scheme (3.6) allows stable calculation up to $t = 7373$ (forced interrupted) with the time step $\Delta t = 0.1$. This test clearly demonstrates that the proposed new scheme is much more robust than the classical semi-implicit Euler-Maruyama scheme.

Table 2 Same as Table 1 but for $G(u) = 5u$

	Semi-implicit		New scheme	
	u_{error}	Order	u_{error}	Order
Time step Δt				
1.00E-4	4.28E-3	-	3.54E-3	-
5.00E-5	2.92E-3	0.55	2.58E-3	0.45
2.50E-5	2.02E-3	0.53	1.76E-3	0.56
1.25E-5	1.47E-3	0.46	1.25E-3	0.49
6.25E-6	1.04E-3	0.50	8.47E-4	0.56
Mesh size h				
1/16	1.04E-2	-	1.04E-2	-
1/32	2.75E-3	1.92	2.69E-3	1.96
1/64	7.12E-4	1.95	6.82E-4	1.98
1/128	1.83E-4	1.96	1.76E-4	1.96
1/256	4.37E-5	2.07	4.28E-5	2.04

Example 4.2 (Phenomenon comparison) In this example, the time evolution of the numerical solution of the stochastic Allen-Cahn equation is compared to that of the deterministic Allen-Cahn equation to show the effect of random perturbations. The deterministic Allen-Cahn equation reads:

$$u_t(x,t) = \triangle u + \frac{u-u^3}{\varepsilon^2}, \quad t \in (0,T), \ x \in D. \tag{4.4}$$

Let $W(x,t)$ be the same as shown in (4.2), $u_0 = \sin(4\pi x)$, $u(x,0) = u(x,1) = 0$, $T = 0.1$, $\Delta t = 10^{-4}$, $h = 1/256$, $\varepsilon = 10^{-2}$, $c_0 = 0$, $\gamma = 1$. We compare the numerical solutions between the stochastic Allen-Cahn equations (4.1) and the deterministic equation (4.4). The contour lines of the computed solutions in the (x,t)-plan are plotted in Fig. 2, in which the stochastic solution is the mean of 30 samples. It is observed from this comparison:

i) compared to the deterministic model, when a random diffusion coefficient field is incorporated, the thickness of the phase field interface is increased, and the interface shifts randomly, as seen from Fig. 2(b);
ii) when force noise is introduced and the diffusion coefficient is deterministic, the kinks interact and annihilate each other, as shown in Fig. 2(c). This is in a good agreement with the result reported in [41].
iii) with both the noise and random diffusion coefficient field, a phenomenon that is a overlay of (i) and (ii) arises, as seen in Fig. 2(d).

We now perform two simulations of phase interface evolution to show the perturbing effects of the random factors on the numerical solution. This is done through numerically solving the two-dimensional Allen-Cahn equation by using the extended Euler-Maruyama scheme. Let $D = (0,1)^2$.

$$W(x,t) := \sum_{i,j=1}^{\infty} \sqrt{q_{ij}} \sin(i\pi x_1) \sin(j\pi x_2) \beta_{ij}(t),$$

where $q_{ij} = \exp(-\frac{i^2+j^2}{200})$ and $\beta_{ij}(t)$ are the i.i.d Brownian motions.

In the deterministic case, it has been known that as $\varepsilon \to 0$, the zero level set of u, denoted by $\Gamma_t^\varepsilon := \{x \in D : u(x,t) = 0\}$, approaches a surface Γ_t whose evolution follows the geometric law:

$$V = -\frac{1}{R} = -\kappa,$$

where V is the normal velocity of the surface Γ_t at each point, κ is its mean curvature, and R is the principal radius of curvature [36, 38]. If we denote the radius at time t by $R(t)$ and set the initial radii to be R_0, then $R(t) = \sqrt{R_0^2 - 2t}$.

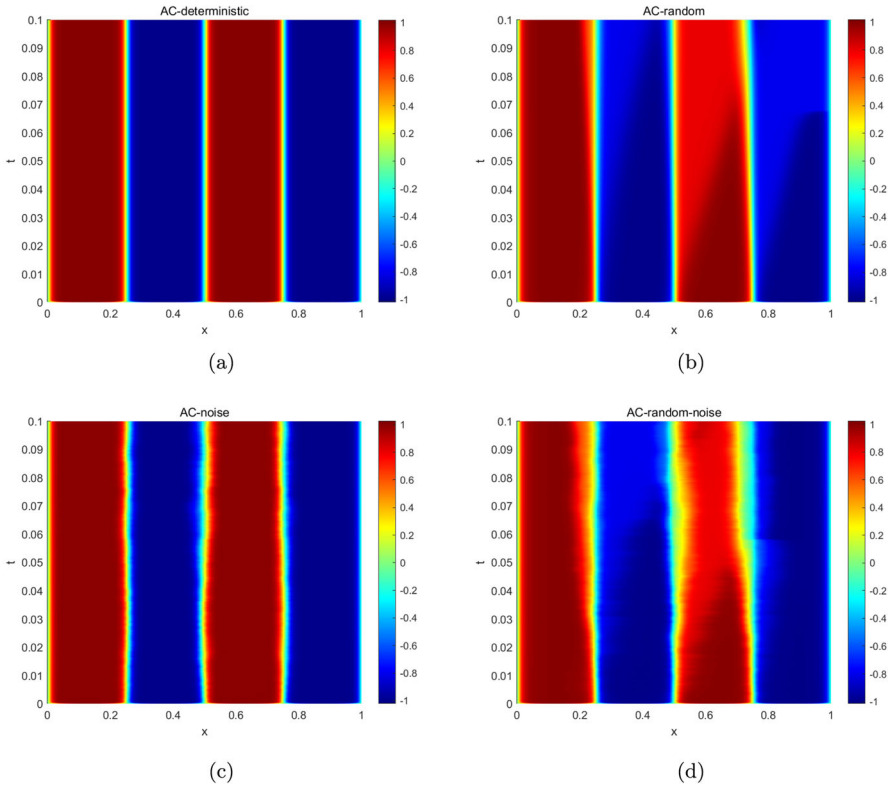

Fig. 2 Comparison of the time evolution of numerical solutions of the one dimensional stochastic and deterministic Allen-Cahn equation. (a) deterministic. (b) random with $q = 2$, $G(u) = 0$. (c) deterministic diffusion coefficient and $G(u) = 5(1 - u^2)$. (d) random with $q = 2$, $G(u) = 5(1 - u^2)$

We simulate double-circle shrinkage evolution using the equation (4.1) with $\varepsilon = 1.5 \times 10^{-3}$, $c_0 = 0$, and the following initial condition:

$$u_0 = \tanh \frac{0.4 - \sqrt{(x_1 - 0.5)^2 + (x_2 - 0.5)^2}}{\sqrt{2}\varepsilon} - \tanh \frac{0.3 - \sqrt{(x_1 - 0.5)^2 + (x_2 - 0.5)^2}}{\sqrt{2}\varepsilon} - 1$$

using 256×256 mesh and the time step $\Delta t = 5 \times 10^{-5}$. Figure 3 shows the evolution of the initial concentration at the times given above each subfigure for both deterministic case and random perturbations. In this figure the first row corresponds to the deterministic case, the remaining rows are for deterministic coefficient with $G(u) = 2(1-u^2)$; $q = 2$, $G(u) = 0$; and $q = 2$, $G(u) = 2(1 - u^2)$ respectively. It is observed that the double-circle shrinks regularly in the deterministic case. However, when the random diffusion coefficient field or noise are added, the shape of the circle evolves irregularly over time, the thickness of the phase field interface thickens, and some small-scale

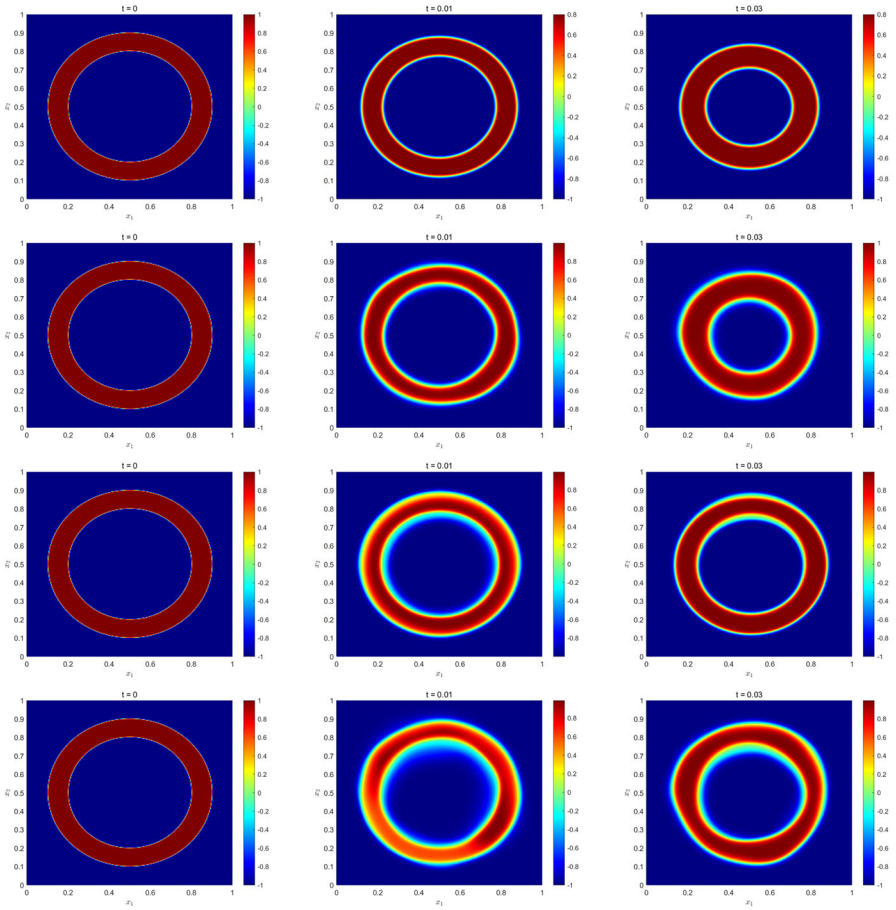

Fig. 3 Interface evolution of a star-shaped at $t = 0, 0.001, 0.005$. The first row: deterministic case. The second row: random case with $q = 2$ and $G(u) = 0$. The third row: deterministic diffusion coefficient and $G(u) = 2(1 - u^2)$. The fourth row: random case with $q = 2$ and $G(u) = 2(1 - u^2)$

structures are generated. Notably, the last row of Fig. 3 shows the cumulative effects of both random diffusion coefficient fields and force noise.

The second simulation is the evolution of a star-shaped curvature-driven interface. We use 10 sample points and 512×512 mesh in this simulation. Set $\varepsilon = 7.5 \times 10^{-4}$, $\Delta t = 5 \times 10^{-5}$, $c_0 = 0$, and the initial condition:

$$\begin{cases} u(x_1, x_2, 0) = \tanh \dfrac{1.5 + 1.2\cos(8\theta) - 2\pi r}{\sqrt{2}\varepsilon}, \\ \theta = \arctan \dfrac{x_2 - 0.5}{x_1 - 0.5}, \\ r = \sqrt{(x_1 - 0.5)^2 + (x_2 - 0.5)^2}. \end{cases}$$

The time evolution of the sample mean of the numerical solutions is presented in Fig. 4. Again we use this simulation to investigate the impact of the randomness. The first row, which corresponds to the deterministic case, confirms the well known results that the tips of the star move inward, while the gaps between the tips move outward, and the whole shape shows a trend of shrinking towards the center. The second row shows the effect of the random diffusion coefficient with $q = 2$, $G(u) = 0$. We observe that the thickness of the interface is expanded, and the evolution of the star interface lost the symmetrical shape due to the diffusion randomness. The third row stands for the case with deterministic diffusion coefficient and $G(u) = 2(1 - u^2)$, from which we see that noise causes small-scale structures, and makes star-shaped interface shifted slightly. The last row of Fig. 4 presents the case where $q = 2$ and $G(u) = 2(1 - u^2)$, which can be seen as a combination of the effects of random factors observed in the

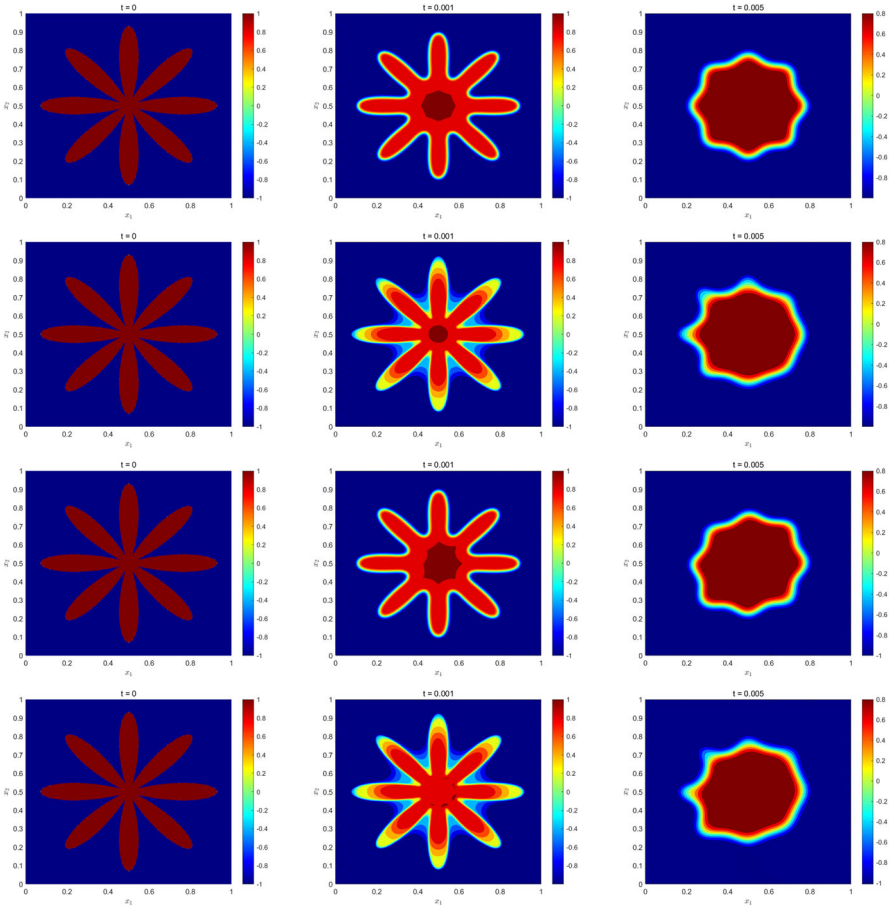

Fig. 4 Interface evolution of the initial double-circle at $t = 0, 0.01, 0.03$. The first row: deterministic case. The second row: deterministic coefficient and $G(u) = 2(1 - u^2)$. The third row: random case with $q = 2$ and $G(u) = 0$. The fourth row: random case with $q = 2$ and $G(u) = 2(1 - u^2)$

second and third rows. The kinks interact, even cancel each other out, and new kinks may appear.

5 Conclusions

In this paper we have considered a stochastic Allen-Cahn equation driven by a bounded log-Whittle-Matérn random diffusion coefficient field and Q-Wiener multiplicative force noise. The well-posedness of the considered equation was established. Basically, the proof of the existence of a mild solution made use of the fixed point theorem, with help of the assumptions imposed on the nonlinear term $G(\cdot)$ and the random coefficient. A number of known results, including the Karhunen-Loève expansion of Q-Wiener process, Ito isometry, and the inequality of the semigroup generated by the stochastic elliptic operator, was used in the proof. For the numerical solution, an efficient time-stepping scheme was proposed, which is an extension of the classical Euler-Maruyama scheme under an auxiliary variable reformulation of the stochastic Allen-Cahn equation. We have showed that the proposed scheme is very efficient since only two decoupled second-order equations with random coefficients need to be solved at each time step. Moreover, the new scheme is unconditionally stable in the sense that a discrete energy is dissipative when the multiplicative noise is absent. Notably, through several numerical examples, we have demonstrated that the new scheme is much more efficient than the classical semi-implicit Euler-Maruyama scheme. Finally, using the proposed scheme, impact of the coefficient randomness and the noise on the phase interface evolution was investigated.

Declarations

Conflict of interest The authors declare no competing interests.

References

1. Allen, S.M., Cahn, J.W.: A microscopic theory for antiphase boundary motion and its application to antiphase domain coarsening. Acta Metall **27**(6), 1085–1095 (1979)
2. Andersson, A., Larsson, S.: Weak convergence for a spatial approximation of the nonlinear stochastic heat equation. Math. Comput **85**(299), 1335–1358 (2016)
3. Babuška, I., Nobile, F., Tempone, R.: A stochastic collocation method for elliptic partial differential equations with random input data. SIAM J Numer Anal **45**(3), 1005–1034 (2007)
4. Babuška, I., Tempone, R., Zouraris, G.E.: Galerkin finite element approximations of stochastic elliptic partial differential equations. SIAM SIAM J Numer Anal **42**(2), 800–825 (2004)
5. Becker, S., Gess, B., Jentzen, A., Kloeden, P.E.: Strong convergence rates for explicit space-time discrete numerical approximations of stochastic Allen-Cahn equations. Stoch. Partial Differ. Equ. Anal Comput 1–58 (2022)
6. Becker, S., Jentzen, A.: Strong convergence rates for nonlinearity-truncated Euler-type approximations of stochastic Ginzburg-Landau equations. Stoch Process Applic **129**(1), 28–69 (2019)
7. Bou-Rabee, N., Vanden-Eijnden, E.: Continuous-time random walks for the numerical solution of stochastic differential equations. Am. Math. Soc. (2018)
8. Bréhier, C.-E., Cui, J., Hong, J.: Strong convergence rates of semidiscrete splitting approximations for the stochastic Allen-Cahn equation. IMA J. Numer. Anal. **39**(4), 2096–2134 (2019)

9. C.-E. Bréhier and L. Goudenège. Analysis of some splitting schemes for the stochastic Allen-Cahn equation. (2018) arXiv:1801.06455
10. Bréhier, C.-E., Goudenège, L.: Weak convergence rates of splitting schemes for the stochastic Allen-Cahn equation. BIT Numer. Math. **60**(3), 543–582 (2020)
11. Cai, M., Gan, S., Wang, X.: Weak convergence rates for an explicit full-discretization of stochastic Allen-Cahn equation with additive noise. J. Sci. Comput. **86**(3), 1–30 (2021)
12. Chopin, N.: Fast simulation of truncated Gaussian distributions. Stat Comput **21**(2), 275–288 (2011)
13. Cui, J., Hong, J.: Strong and weak convergence rates of a spatial approximation for stochastic partial differential equation with one-sided Lipschitz coefficient. SIAM J. Num. Anal. **57**(4), 1815–1841 (2019)
14. Cui, J., Hong, J., Liu, Z.: Strong convergence rate of finite difference approximations for stochastic cubic Schrödinger equations. J. Differ. Equ. **263**(7), 3687–3713 (2017)
15. Cui, J., Hong, J., Liu, Z., Zhou, W.: Strong convergence rate of splitting schemes for stochastic nonlinear Schrödinger equations. J. Differ. Equ. **266**(9), 5625–5663 (2019)
16. Cui, J., Hong, J., Sun, L.: Semi-implicit energy-preserving numerical schemes for stochastic wave equation via SAV approach. (2022) arXiv:2208.13394
17. Da Prato, G., Jentzen, A., Röckner : A mild itô formula for SPDEs. Trans Am Math Soc **372**(6), 3755–3807 (2019)
18. Da Prato, G., Zabczyk, J.: Stochastic equations in infinite dimensions. Cambridge University Press (2014)
19. Dietrich, C.R.: A simple and efficient space domain implementation of the turning bands method. Water Resour. Res. **31**(1), 147–156 (1995)
20. Dietrich, C.R., Newsam, G.N.: Fast and exact simulation of stationary Gaussian processes through circulant embedding of the covariance matrix. SIAM J. Sci Comput **18**(4), 1088–1107 (1997)
21. Engel, K., Nagel, R.: One-parameter semigroups for linear evolution equations. Semigr Forum **63**, 278–280 (1999)
22. Feng, X., Li, Y., Zhang, Y.: Finite element methods for the stochastic Allen-Cahn equation with gradient-type multiplicative noise. SIAM J. Num Anal **55**(1), 194–216 (2017)
23. Gohberg, I., Goldberg, S., Kaashoek, M.A.: Hilbert-schmidt operators. Classes of Linear Operators Vol. I, pp. 138–147. Springer, (1990)
24. Hausenblas, E.: Approximation for semilinear stochastic evolution equations. Potential Anal **18**(2), 141–186 (2003)
25. Hutzenthaler, M., Jentzen, A.: Numerical approximations of stochastic differential equations with non-globally Lipschitz continuous coefficients, vol. 236. American Mathematical Society, (2015)
26. Hutzenthaler, M., Jentzen, A.: On a perturbation theory and on strong convergence rates for stochastic ordinary and partial differential equations with nonglobally monotone coefficients. Ann. Prob. **48**(1), 53–93 (2020)
27. Hutzenthaler, M., Jentzen, A., Kloeden, P.E.: Strong and weak divergence in finite time of Euler's method for stochastic differential equations with non-globally Lipschitz continuous coefficients. Proc. Math. Phys. Eng. Sci. **467**(2130), 1563–1576 (2011)
28. Jentzen, A., Pušnik, P.: Strong convergence rates for an explicit numerical approximation method for stochastic evolution equations with non-globally Lipschitz continuous nonlinearities. IMA J. Num. Anal. **40**(2), 1005–1050 (2020)
29. Johnson, N.L., Kotz, S., Balakrishnan, N.: Continuous univariate distributions, volume 289. John Wiley & Sons, (1995)
30. Kazashi, Y.: Quasi-Monte Carlo integration with product weights for elliptic PDEs with log-normal coeffcients. IMA J. Num. Anal. **39**(3), 1563–1593 (2019)
31. Kloeden, P.E., Platen, E.: Numerical solution of stochastic differential equations. Springer Science and Business Media, (2013)
32. Kovács, M., Larsson, S., Lindgren, F.: On the backward Euler approximation of the stochastic Allen-Cahn equation. J Appl. Prob. **52**(2), 323–338 (2015)
33. Kovács, M., Larsson, S., Lindgren, F.: On the discretisation in time of the stochastic Allen-Cahn equation. Math. Nachrichten **291**(5–6), 966–995 (2018)
34. Kruse, R.: Optimal error estimates of Galerkin finite element methods for stochastic partial differential equations with multiplicative noise. IMA J. Numer. Anal. **34**(1), 217–251 (2014)
35. Kruse, R.: Strong and weak approximation of semilinear stochastic evolution equations. Springer, (2014)

36. Li, C., Huang, Y., Yi, N.: An unconditionally energy stable second order finite element method for solving the Allen-Cahn equation. J. Comput. Appl. Math. **353**, 38–48 (2019)
37. Li, N., Meng, B., Feng, X., Gui, D.: The spectral collocation method for the stochastic Allen-Cahn equation via generalized polynomial chaos. Numer. Heat Transf. B: Fundam. **68**(1), 11–29 (2015)
38. Li, Y., Lee, H.G., Jeong, D., Kim, J.: An unconditionally stable hybrid numerical method for solving the Allen-Cahn equation. Comput. Math. Appl. **60**(6), 1591–1606 (2010)
39. Liu, Z., Qiao, Z.: Strong approximation of monotone stochastic partial differential equations driven by white noise. IMA J. Num. Anal. **40**(2), 1074–1093 (2020)
40. Liu, Z., Qiao, Z.: Strong approximation of monotone stochastic partial differential equations driven by multiplicative noise. Stoch. Partial Differ. Equ. Anal Comput **9**(3), 559–602 (2021)
41. Lord, G.J., Powell, C.E., Shardlow, T.: An introduction to computational stochastic PDEs. Cambridge University Press, (2014)
42. Majee, A.K., Prohl, A.: Optimal strong rates of convergence for a space-time discretization of the stochastic Allen-Cahn equation with multiplicative noise. Comput. Methods Appl. Math. **18**(2), 297–311 (2018)
43. Mantoglou, A., Wilson, J.L.: The turning bands method for simulation of random fields using line generation by a spectral method. Water Resour Res **18**(5), 1379–1394 (1982)
44. Milstein, G.N., Tretyakov, M.V.: Stochastic numerics for mathematical physics. Springer Science and Business Media, (2013)
45. Qi, R., Wang, X.: Optimal error estimates of Galerkin finite element methods for stochastic Allen-Cahn equation with additive noise. J Sci. Comput. **80**(2), 1171–1194 (2019)
46. Qi, X., Azaiez, M., Huang, C., Xu, C.: An efficient numerical approach for stochastic evolution PDEs driven by random diffusion coefficients and multiplicative noise. AIMS Math. **7**(12), 20684–20710 (2022)
47. Sauer, M., Stannat, W.: Lattice approximation for stochastic reaction diffusion equations with one-sided Lipschitz condition. Math. Comput. **84**(292), 743–766 (2015)
48. Shen, J., Xu, J., Yang, J.: The scalar auxiliary variable (SAV) approach for gradient flows. J. Comput. Phys. **353**, 407–416 (2018)
49. Shen, J., Yang, X.: Numerical approximations of Allen-Cahn and Cahn-Hilliard equations. Discrete Contin. Dyn. Syst. **28**(4), 1669 (2010)
50. Shinozuka, M.: Simulation of multivariate and multidimensional random processes. J. Acoust. Soc. Am. **49**(1B), 357–368 (1971)
51. Shinozuka, M., Jan, C.-M.: Digital simulation of random processes and its applications. J. Sound Vib. **25**(1), 111–128 (1972)
52. Wadsworth, J.L., Tawn, J.A.: Efficient inference for spatial extreme value processes associated to log-Gaussian random functions. Biometrika **101**(1), 1–15 (2014)
53. Wang, X.: Strong convergence rates of the linear implicit Euler method for the finite element discretization of SPDEs with additive noise. IMA J. Numer. Anal. **37**(2), 965–984 (2017)
54. Wang, X.: An efficient explicit full discrete scheme for strong approximation of stochastic Allen–Cahn equation. (2018) arXiv:1802:09413
55. Wang, X.: An efficient explicit full-discrete scheme for strong approximation of stochastic Allen-Cahn equation. Stoch. Process. Their Appl **130**(10), 6271–6299 (2020)
56. Wood, A.T.A., Chan, G.: Simulation of stationary Gaussian processes in $[0, 1]^d$. J. Comput. Graph. Stat. **3**(4), 409–432 (1994)
57. Yan, Y.: Galerkin finite element methods for stochastic parabolic partial differential equations. SIAM J. Numer. Anal. **43**(4), 1363–1384 (2005)
58. Zhang, Z., Karniadakis, G.: Numerical methods for stochastic partial differential equations with white noise. Springer International Publishing, (2017)